Cytometry PART A
Journal of the International Society for Advancement of Cytometry

MIFlowCyt

Fluorescence-Free Flow Cytometry for Measurement of Shape Index Distribution of Resting, Partially Activated, and Fully Activated Platelets

A.L. Litvinenko,[1,2] A.E. Moskalensky,[1,2] N.A. Karmadonova,[3] V.M. Nekrasov,[1,2] D.I. Strokotov,[1,4] A.I. Konokhova,[1] M.A. Yurkin,[1,2] E.A. Pokushalov,[3] A.V. Chernyshev,[1,2] V.P. Maltsev[1,2,4]*

[1]Voevodsky Institute of Chemical Kinetics and Combustion, Novosibirsk, Russian Federation

[2]Novosibirsk State University, Novosibirsk, Russian Federation

[3]State Research Institute of Circulation Pathology, Novosibirsk, Russian Federation

[4]Novosibirsk State Medical University, Novosibirsk, Russian Federation

Received 5 May 2016; Revised 1 September 2016; Accepted 5 October 2016

Grant sponsor: Russian Science Foundation, Grant number: 14-15-00155

Grant sponsor: Russian Foundation for Basic Research (Supercomputer calculations), Grant number: 16-34-00228

Additional Supporting Information may be found in the online version of this article.

*Correspondence to: Valeri P. Maltsev, Institutskaya 3, Novosibirsk, 630090, Russian Federation. E-mail: maltsev@kinetics.nsc.ru

Published online 00 Month 2016 in Wiley Online Library (wileyonlinelibrary.com)

DOI: 10.1002/cyto.a.23003

Abstract

Whereas commercially available hematological analyzers measure volume of individual platelets, angle-resolved light-scattering provides unique ability to additionally measure their shape index. We utilized the scanning flow cytometer to measure light-scattering profiles (LSPs) of individual platelets taken from 16 healthy donors and the solution of the inverse light-scattering problem to retrieve the volume and shape index of each platelet. In normal conditions, the platelet shape index distribution (PSID) demonstrates three peaks, which relate to resting, partially activated, and fully activated platelets. We developed an algorithm, based on fitting PSID by a sum of three peak functions, to determine the percentage, mean platelet shape index, and distribution width of each platelet fraction. In total, this method gives eight additional parameters of platelet morphology and function to be used in clinical hematological analysis. We also stimulated the platelets with adenosine diphosphate (ADP) and measured the dependence of equilibrium PSID, including the total percentage of activated platelets, on ADP concentration.

Key terms

platelet shape; flow cytometry; light scattering; platelet activation

Blood platelets are small cells of great importance in many pathophysiological processes including thrombosis, hemorrhage, inflammation, wound healing, antimicrobial host defense, angiogenesis, and tumor growth and metastasis (1). Therefore, the platelets should be characterized with as much details as possible in the framework of routine clinical analysis of blood cells. Unfortunately, hematological analyzers measure only individual platelet volume with either electrical-impedance or two-angle light-scattering methods (2). Together with platelet counting, this results in only four basic parameters of platelet population (three of them are independent): the platelet concentration (PLT), the fraction of the blood volume occupied by platelets (plateletcrit, PCT), the mean platelet volume (MPV), and the (PDW). Both methods ignore shape differences between measured cells introducing uncontrolled errors in determination of single platelet volume. Manufacturers of hematological analyzers are trying to provide additional parameters using low-angle light scattering and fluorescence from biomarkers (3). In particular, fluorescence of RNA-linked dyes used to determine of immature platelet fraction (IPF) (4). However, the immature fraction is separated from normal cells by a somewhat arbitrarily placed line that, again, results in uncontrolled errors of IPF (5). Whereas fluorescent markers require more complicated and expensive sample preparation, the light-scattering intensities measured at two solid angles (forward and side scattering) in ordinary

ISAC
International Society for Advancement of Cytometry

flow cytometer do not allow one to determine characteristics of nonspherical particles. Forward and side light-scattering intensities can potentially be used to characterize only single homogeneous spherical particle by its size and refractive index (6). However, the platelet shape is far from a sphere even for activated cells. Hence, an instrumental solution for precise characterization of platelets, including their shape, has to measure larger amount of light-scattering data for each particle. An example of such solution is a scanning flow cytometer (SFC) (7), which measures angle-resolved light-scattering profiles (LSPs) of single particles. It has been used to perform precise characterization of single platelets, including determination of volume (with sub-diffraction precision) and shape (aspect ratio), assuming an oblate spheroid as its optical model (8). Moreover, scanning flow cytometry demonstrated sensitivity to platelet activation accompanied by platelet shape change. The latter is considered an universal indicator of platelet activation (9,10) and several attempts were made to assess this change using forward and side scattering channels (11,12). However, at its best such approach may only be used to detect shape change of population, but not of single cells. From physical point of view, shape change constitutes the disk-to-sphere transformation and pseudopodia formation, which can be characterized by the decrease of cell mean aspect ratio from 4–6 (flat, discoid cells) to 1–2 (rounded cells) (13,14). Note that small size and refractive index of platelets hinder the determination of aspect ratio by optical microscopy (15).

In this article, we used a SFC to measure LSPs of individual platelets and solved the inverse light-scattering (ILS) problem to retrieve volume and shape index of a platelet modelled by an oblate spheroid. The distributions over the platelet shape index were constructed for a number of donors. We fitted them by a sum of three beta density functions to retrieve parameters of resting, partially and fully activated platelets – three fractions which were previously observed by scanning electron microscope (16,17) and fluorescence flow cytometry (18). The developed method allowed us to determine 8 new platelet parameters, which should improve the platelet-related sensitivity of routine blood tests. To illustrate the performance of the new method, we studied an effect of adenosine diphosphate (ADP) stimulation on platelet parameters.

Methods

Scanning Flow Cytometry

The actual SFC measures angle-resolved light scattering in a form of LSP for individual particles with a 660-nm laser which beams parallel to the cell flow and with original light collection system (7,19). Also the 488-nm laser is used to produce forward and side scattering signals in a conventional manner. The instrument used in the present work was fabricated by Cytonova LLC (Novosibirsk, Russia). The LSP strongly depends on the particle morphology, and its potential in precise characterization of blood platelets (8,20) and other cells (21–25) has been demonstrated. Solving the ILS problem, we determine the volume and shape index for each cell in a sample and construct distribution of platelet population over these characteristics.

Sample Preparation

Platelets were obtained from the venous blood of healthy donors with informed consent. Blood was collected using vacuum tubes with sodium citrate. To get the platelet-rich plasma, we followed the guidelines including the sedimentation of red blood cells during approximately 1 hour (26). Several platelet samples were made by 30-fold dilution of plasma with 0.9% saline in plastic tubes. Tubes were allowed to rest for at least 15 min. Each platelet sample was then measured with the SFC either *as is* or after the addition of ADP. The delay between the addition of ADP and measurement was about 30 s. All manipulations were carried out at room temperature (25°C).

Inverse Light-Scattering Problem

To characterize individual platelets from LSPs, we solved the ILS problem applying an oblate spheroid as an optical model for both resting and activated platelets. The solution is based on comparison of a platelet LSP measured by SFC with a spheroid LSP from a theoretically calculated database (8). The characteristics of measured platelet are assumed equal to the characteristics of spheroid (equi-volume sphere diameter d, refractive index n, orientation angle β, and shape index δ) that gave the best-fit for the corresponding measured LSP. An oblate spheroid is the simplest optical model of a platelet, still it gives good agreement of theoretical and experimental LSPs, as well as good precision of determined cell characteristics. Moreover, it works well even for a platelet with pseudopodia, since the latter are much thinner than the wavelength and has little effect on LSP (27).

In our previous study (8) we described a platelet shape via an aspect ratio that is a/b where a and b are the major and minor axes of an oblate spheroid respectively. In the current study, we describe a platelet shape via the following shape index δ:

$$\delta = \frac{2ab}{a^2 + b^2} \tag{1}$$

The shape index of 1 corresponds to a spherical shape (activated platelet) whereas shape index of 0.1 corresponds to a discoid (resting platelet) with aspect ratio of approximately 20. Note that δ is the harmonic mean of the aspect ratio and its inverse; thus, it is limited to a range [0,1]. Moreover, as shown below, it has some favorable properties in terms of the resulting distributions.

In total, we used four spheroid characteristics: equi-volume sphere diameter d, refractive index n, orientation angle β, and shape index δ. The theoretical database with 2,00,000 records containing spheroid characteristics and corresponding LSPs was constructed by randomly sampling characteristics from the following intervals: $d \in [1.0\ \mu\text{m}, 4.24\ \mu\text{m}]$, $n \in [1.37, 1.39]$, $\beta \in [0°, 90°]$, $\delta \in [0.1, 1]$, based on literature data (14,15,28,29). Theoretical LSPs were calculated at the Supercomputing center of the Novosibirsk State University

using the code ADDA v.1.2 (30), based on the discrete dipole approximation.

Shape Index Distribution Analysis

The solution of the ILS problem allows one to determine four characteristics of each platelet measured with the SFC, but only two of them (volume and shape index) have clinical importance. The other characteristics of a platelet (refractive index and orientation angle) play a technical role in solution of the ILS problem. Distribution over platelet volume is an established component of a clinical analysis and is commonly described by MPV and PDW parameters (31). The distribution over the platelet shape index has not been previously measured with sufficient statistics. Below we introduce a new algorithm for analysis of this distribution.

We propose the following scaled beta (distribution) density function (32) for analysis of platelet shape index distribution (PSID):

$$f(\delta;\delta_{\min},\delta_{\max},\delta_0,\gamma)=\begin{cases}\dfrac{x^{\alpha-1}(1-x)^{\gamma-1}}{\mathrm{B}(\alpha,\gamma)(\delta_{\max}-\delta_{\min})}, & 0\le x\le 1;\\ 0, & \text{otherwise.}\end{cases}$$

$$x=\frac{\delta-\delta_{\min}}{\delta_{\max}-\delta_{\min}},\ \alpha=1+(\gamma-1)\frac{\delta_0-\delta_{\min}}{\delta_{\max}-\delta_0}, \tag{2}$$

where $\mathrm{B}(\alpha,\gamma)$ is the Euler beta function, $\delta_{\min}$ and $\delta_{\max}$ are left and right boundary values, at which density falls to zero, and δ_0 is the peak location (mode). This function is normalized to have unit integral over the whole range of δ, and can represent both symmetric and asymmetric distributions. Parameter $\gamma>1$ is responsible for the degree of curvature (kurtosis) of the function, while the asymmetry is quantitatively described by the ratio $(\delta_0-\delta_{\min})/(\delta_{\max}-\delta_0)$. For $\gamma>2$ $(\alpha>2)$ the function approaches its right (left) boundary value smoothly (with zero derivative); otherwise, its derivative is not continuous at the corresponding boundary.

The mean value of the beta distribution is given as

$$E[\delta]=\delta_0+\frac{(\delta_{\max}-\delta_0)(\delta_{\max}+\delta_{\min}-2\delta_0)}{\gamma(\delta_{\max}-\delta_{\min})+\delta_{\max}+\delta_{\min}-2\delta_0}, \tag{3}$$

which is exactly δ_0 in the symmetric case. The full width at half maximum (FWHM) can be evaluated by solving the following equation:

$$x^{\frac{\delta_0-\delta_{\min}}{\delta_{\max}-\delta_0}}(1-x)=\left(\frac{1}{2}\right)^{\frac{1}{\gamma-1}}\left(\frac{\delta_0-\delta_{\min}}{\delta_{\max}-\delta_{\min}}\right)^{\frac{\delta_0-\delta_{\min}}{\delta_{\max}-\delta_0}}\frac{\delta_{\max}-\delta_0}{\delta_{\max}-\delta_{\min}}, \tag{4}$$

which has exactly two solutions in the range (0,1): x_1 and x_2. The FWHM is then given as $w=|x_1-x_2|(\delta_{\max}-\delta_{\min})$. For important case of symmetric beta density, Eq. (4) boils down to a trivial quadratic equation implying

$$w=(\delta_{\max}-\delta_{\min})\sqrt{1-\left(\frac{1}{2}\right)^{\frac{1}{\gamma-1}}} \tag{5}$$

Based on our results and literature data (16–18), we account for three platelet fractions – resting (index "r"), partially activated (index "pa"), and fully activated platelets (index "fa"). Among a multitude of peak functions we have chosen the beta density because it vanishes at the boundaries of the shape index range, which agrees with natural physical constraints. However, the overall variety of this function family is probably too large, when a sum of three is used to fit a single distribution. So we additionally postulated a number of reasonable constraints. First, we set $\delta_{\min}=0.1$ (corresponding to aspect ratio 20) for resting platelets, which amply covers the physiological range (14) and agrees with the database range, described in section "Inverse light-scattering problem". However, setting $\delta_{\min}=0$ also works fine and has only minor effect on the final results (data not shown). Second, we set $\delta_{\max}=1$ for fully activated platelets, since we did not find any spherical platelets when applied the algorithm for separation of spherical and spheroidal particles from LSPs (33). Third, we assumed that distributions of both resting and fully activated platelets are symmetric, since our data gives no reliable indications against it. Finally, acknowledging our lack of knowledge about the partially activated fraction, we set the support of the corresponding beta density to the whole range, i.e., $\delta_{\min}=0.1$ and $\delta_{\max}=1$. Then we have to allow it to be nonsymmetric not to fix the peak position δ_0.

To conclude, the measured PSID are fitted by the following normalized function:

$$f_\Sigma(\delta)=\eta_{\mathrm{r}}\times f(\delta;0.1,2\delta_0^{\mathrm{r}}-0.1,\delta_0^{\mathrm{r}},\gamma_{\mathrm{r}})+\eta_{\mathrm{fa}}\times f(\delta;2\delta_0^{\mathrm{fa}}-1,1,\delta_0^{\mathrm{fa}},\gamma_{\mathrm{fa}})+(1-\eta_{\mathrm{r}}-\eta_{\mathrm{fa}})\times f(\delta;0.1,1,\delta_0^{\mathrm{pa}},\gamma_{\mathrm{pa}}), \tag{6}$$

where η_{r} and η_{fa} are to percentages of resting and fully activated platelets, respectively. The fitting function contains eight unknown parameters, including peak positions and width-related parameter for three platelet fractions, plus one additional scaling coefficient, if the processed distribution (histogram) is not normalized (see, e.g., Fig. 1). To provide an adequate precision in determination of these parameters, one should construct the PSID with >30 bins and a maximal bin of about 300 cells. Thus, we recommend measuring >5000 platelets in each sample.

Analysis of ADP Stimulus

In analysis of ADP stimulus on platelet activation, we used a simple empirical function based the assumption that the increase of total percentage of activated platelets $\eta_{\mathrm{a}}=1-\eta_{\mathrm{r}}$ is proportional to the average amount of ADP molecules bound to platelets. The binding of ADP can be described by the following kinetic scheme (34):

$$\mathrm{ADP}+\mathrm{R}\overset{K}{\leftrightarrow}\mathrm{ADP}\cdot\mathrm{R}, \tag{7}$$

where R denotes the ADP receptor $\mathrm{P2Y}_1$ (35) and K is the equilibrium constant. Since our experimental conditions correspond to excess of ADP, scheme (7) and the above assumption lead to the following dependency of η_{a} on ADP concentration:

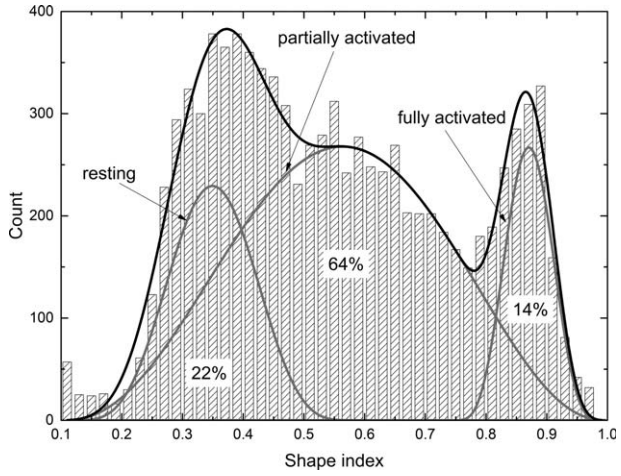

Figure 1. Typical PSID, corresponding to donor #6. Also shown is the best-fit of the PSID by approximating function (black line) and its components for resting, partially and fully activated platelet fractions (grey lines and percentages).

$$\eta_a = \eta_0 + \frac{(\eta_{max} - \eta_0) \cdot [ADP]}{K + [ADP]}, \qquad (8)$$

where η_0 is the initial and η_{max} – the maximum possible percentage of activated platelets (determined by total ADP receptors). This equation was used to retrieve K from experiments.

Results

Platelet Shape Index Distribution

In contrast to an ordinary flow cytometer, the SFC collects larger amount of light-scattering information, which enables precise determination of platelet shape index, construction of PSID, and consequent differentiation of three platelet populations (Fig. 1). The PSID shown in Figure 1 is typical in analysis of platelets with SFC together with the fit by Eq. (6) and corresponding percentages of resting, partially, and fully activated platelets. Based on the fit, we propose the following hematological parameters to characterize a platelet population in blood: %RP and %FAP are the percentages of resting (η_r), and fully activated platelets (η_{fa}); MPSI-R, MPSI-FA, and MPSI-PA are the mean platelet shape index for resting (δ_0^r), fully activated (δ_0^{fa}), and partially activated [calculated with Eq. (3)] fractions, respectively; PSIDW-R, PSIDW-FA, and PSIDW-PA are platelet-shape-index distribution widths for resting (w_r), fully activated (w_{fa}), and partially activated (w_{pa}) fractions, respectively. Widths w_r and w_{fa} are obtained with Eq. (5), while w_{pa} – through the solution of Eq. (4). Combined with three standard platelets parameters, PLT, MPV and PDW, the developed method provides total of 11 parameters for routine analysis of platelets.

To illustrate the performance of the method, we measured platelets of 16 donors. The percentage for resting platelets in the samples varied from 4% to 43%. The resulting parameters are summarized in Table 1, where we have also included η_a for convenience. The typical scatterplots and

Table 1. Platelet parameters measured with scanning flow cytometry for 16 donors

#	RESTING PLATELETS			ACTIVATED PLATELETS								
				PARTIALLY ACTIVATED		FULLY ACTIVATED						
	MPSI-R	PSIDW-R	%PR	MPSI-PA	PSIDW-PA	MPSI-FA	PSIDW-FA	%PFA	η_a, %	MPV, fl	PDW, fl	PLT, 10^6/ml
1	0.347 ± 0.012	0.16 ± 0.02	15 ± 2	0.605 ± 0.008	0.31 ± 0.05	0.873 ± 0.005	0.166 ± 0.008	29 ± 3	85 ± 2	10.2 ± 0.5	8.6	246
2	0.309 ± 0.006	0.16 ± 0.03	12.5 ± 1.6	0.69 ± 0.02	0.36 ± 0.04	0.900 ± 0.004	0.160 ± 0.016	14 ± 4	87.5 ± 1.6	10.0 ± 0.6	10.0	223
3	0.357 ± 0.009	0.09 ± 0.03	7 ± 2	0.60 ± 0.06	0.55 ± 0.05	0.891 ± 0.007	0.13 ± 0.04	13 ± 4	93 ± 2	7.8 ± 7	8.5	268
4	0.396 ± 0.010	0.09 ± 0.04	9 ± 3	0.619 ± 0.018	0.48 ± 0.02	0.92 ± 0.03	0.12 ± 0.10	1 ± 1	91 ± 3	8.3 ± 0.8	9.2	251
5	0.313 ± 0.005	0.17 ± 0.03	43 ± 15	0.52 ± 0.08	0.43 ± 0.12	0.87 ± 0.02	0.14 ± 0.07	7 ± 3	57 ± 15	11.7 ± 1.7	10.6	277
6	0.350 ± 0.006	0.17 ± 0.03	22 ± 8	0.56 ± 0.03	0.43 ± 0.07	0.870 ± 0.003	0.093 ± 0.015	13.9 ± 1.8	78 ± 8	6.34 ± 0.14	11.5	212
7	0.339 ± 0.006	0.18 ± 0.03	28 ± 9	0.56 ± 0.04	0.41 ± 0.08	0.880 ± 0.004	0.094 ± 0.014	13.0 ± 1.9	72 ± 9	6.04 ± 0.15	11.7	224
8	0.309 ± 0.005	0.150 ± 0.015	28 ± 5	0.58 ± 0.02	0.41 ± 0.06	0.908 ± 0.012	0.11 ± 0.05	6 ± 2	72 ± 5	12.0 ± 1.4	8.6	279
9	0.362 ± 0.009	0.129 ± 0.010	35 ± 4	0.601 ± 0.010	0.50 ± 0.13	0.865 ± 0.009	0.139 ± 0.014	17 ± 2	65 ± 4	10.3 ± 2.9	10.4	238
10	0.251 ± 0.018	0.19 ± 0.06	9 ± 3	0.560 ± 0.013	0.43 ± 0.03	0.908 ± 0.005	0.139 ± 0.015	11.2 ± 1.5	91 ± 3	12.2 ± 1.3	10.4	231
11	0.298 ± 0.010	0.08 ± 0.03	4 ± 2	0.527 ± 0.014	0.46 ± 0.03	0.900 ± 0.004	0.15 ± 0.06	4 ± 2	96 ± 2	11.1 ± 0.9	10.3	246
12	0.298 ± 0.005	0.052 ± 0.016	4.2 ± 1.3	0.518 ± 0.013	0.54 ± 0.05	0.886 ± 0.005	0.144 ± 0.015	15.9 ± 1.6	95.8 ± 1.3	6.9 ± 0.2	7.3	218
13	0.34 ± 0.03	0.11 ± 0.05	4 ± 3	0.56 ± 0.09	0.73 ± 0.05	0.87 ± 0.02	0.16 ± 0.07	7 ± 6	96 ± 3	9.1 ± 0.2	7.8	255
14	0.336 ± 0.014	0.15 ± 0.02	10 ± 3	0.57 ± 0.07	0.66 ± 0.12	0.926 ± 0.004	0.100 ± 0.014	12 ± 3	90 ± 3	6.39 ± 0.19	8.1	261
15	0.35 ± 0.02	0.25 ± 0.02	12 ± 3	0.75 ± 0.04	0.23 ± 0.04	0.897 ± 0.010	0.110 ± 0.011	16 ± 9	88 ± 3	11 ± 1	8.1	220
16	0.35 ± 0.05	0.25 ± 0.02	23 ± 12	0.59 ± 0.05	0.32 ± 0.02	0.891 ± 0.007	0.162 ± 0.018	16 ± 2	77 ± 12	8.98 ± 0.14	6.5	251

All fitted parameters are given as best-fit value ± standard deviation; the data for MPV is mean ± standard error of mean.

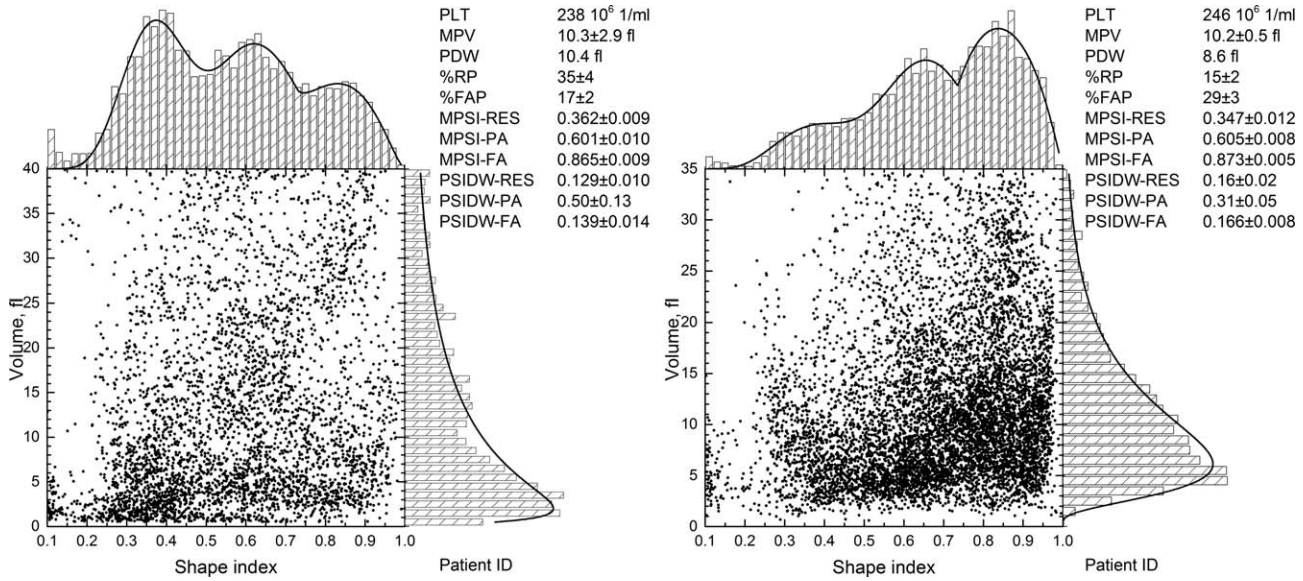

Figure 2. Scatterplot of platelet volume versus shape index for donors #9 (left) and #1 (right), distributions over both characteristics, and 11 parameters of platelet population.

distributions over platelet volume and shape index are shown in Figure 2 (for donor #9 and #1).

Evolution of PSID in Response to ADP

The ADP stimulation caused a rapid drop of percentage of resting platelets (36) that was further stable for at least10 min. To quantify the effect of ADP stimulus, we measured PSIDs of 10 samples of one donor as described in Methods after stimulation by different doses of ADP starting from 20 μM and dividing by 2 down to 0.08 μM. These 10 PSIDs were processed the same way as other samples to determine η_a, among other parameters, for each sample. Three example PSIDs, unstimulated and stimulated by two different doses, are shown in Figure 3 together with fit results. Dependence of determined η_a on these nine ADP doses is presented in Figure 4. We fitted it by Eq. (8) and obtained the equilibrium constant $K = (8 \pm 2) \times 10^{-8}$ M.

Discussion

We introduced definition of the shape index of oblate spheroid in the form of Eq. (1) because such definition provides approximately equal peak widths for resting and fully activated platelets (see Figs. 1 and 2, parameters PSIDW-R and PSIDW-FA in Table 1). We have also tried definitions related to the aspect ratio (8), sphericity (37), and volume sphericity index (38). However, they resulted in distributions with largely different widths of components, which is inconvenient for further processing using the uniform binning of the underlying histogram. Let us further reflect on the choice of the peak function. It may seem that unrestricted beta density has too many free parameters, given the data to fit. However, after the additional constraints, each peak is described by only two parameters (position and width), not accounting for relative amplitudes. Thus, it is the minimum possible number of

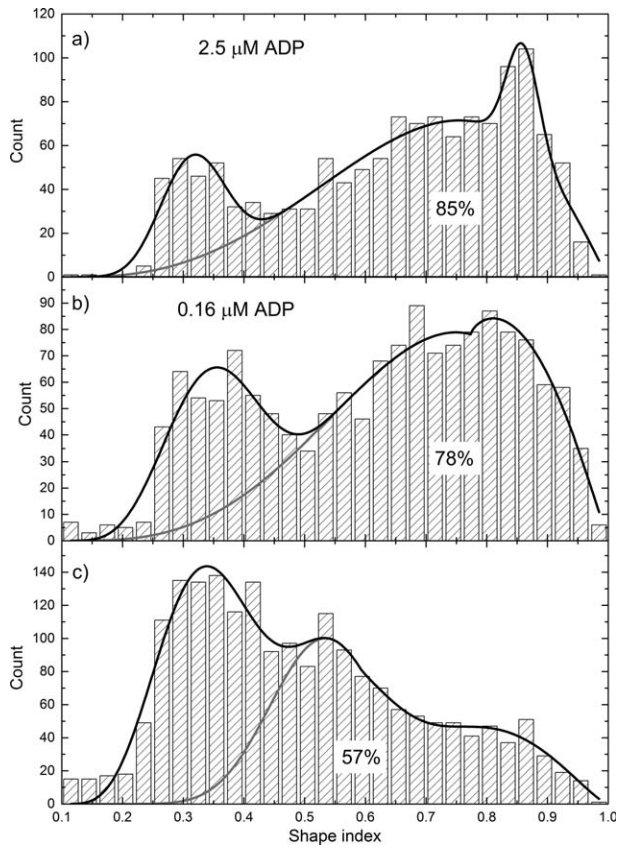

Figure 3. Distribution of platelets over shape index for samples of the same donor stimulated by 2.5 μM (**a**) and 0.16 μM (**b**) ADP and unstimulated (**c**). Also shown are the best-fit approximating functions (black lines) and its activated component (sum of partially and fully activated fraction, grey lines) together with percentage η_a.

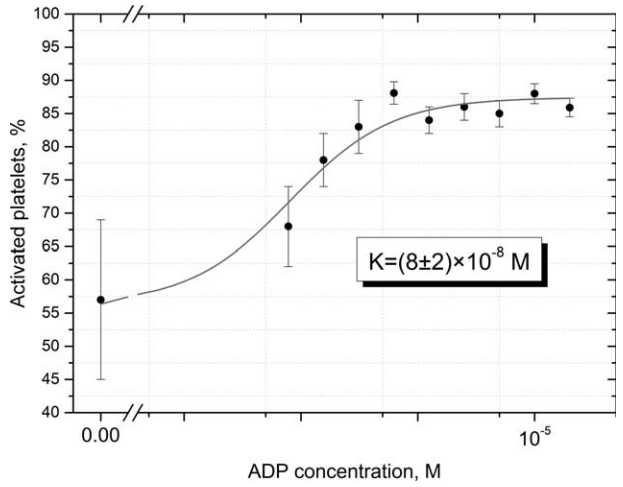

Figure 4. The percentage of activated platelets as a function of ADP doses. The PSID of ADP doses of 0, 0.16, and 2.5 μM are shown in Figure 3. The line corresponds to the best-fit of experimental points by the molecular-kinetic model based on ligand-receptor binding. Resulting equilibrium constant for ADP-platelet binding is also shown (best fit value ± standard deviation).

parameters, equal to, e.g., that for a Gaussian description of the peaks. While the beta density satisfies the physical requirement of zero boundary values, it is still only a convenient empiric function. The wealth of information provided by the measured PSID allows one, in principle, to develop more realistic theoretical description of this distribution – an important topic for future research. However, this can only be done based on understanding of molecular mechanisms underlying the platelet shape change based, e.g., on the geometry of the ring of microtubules and its evolution during the activation (39,40).

We noticed that in some cases, a PSID could be also fitted by a sum of only two beta densities, e.g., donors #4 and #13 in Table 1 and Figure 2(b). However, the standard procedure also works fine, while the possible ambiguity is indicated by large relative uncertainties of parameters of fully activated platelets (%PFA and PSIDW-FA). Overall, the platelet parameters in Table 1 demonstrate different magnitudes of variations. In particular, MPSI-R varies from 0.251 to 0.396 (mean value 0.332), PSIDW-R—from 0.05 to 0.25, %RP—from 4% to 43%, MPSI-PA—from 0.52 to 0.75 (mean value 0.59), PSIDW-PA—from 0.23 to 0.73, MPSI-FA—from 0.865 to 0.926 (mean value 0.891), PSIDW-FA—from 0.09 to 0.17, %FAP—from 1% to 29%.

We must stress, however, that apart from actual patient platelet characteristics these variations can be caused by manipulations with blood samples before analysis. We tried to follow the standard sampling procedure described in Methods as strictly as possible. Nevertheless, our experience shows that platelet shape (or activation status) is very sensitive to a procedure of taking blood sample using a steel needle, transportation of blood sample from patient to the analyzer, and platelet flow in thin plastic tubes of the flow cytometer (data not shown), in accordance with other researchers (41). This fact forces us to optimize the preanalytical procedure for analysis of platelet parameters with the new method. The goal is to reduce manipulations of a blood sample as much as possible.

We presented the first attempt to apply the new method to analysis of ADP stimulus on platelet activation. The PSIDs are sensitive to ADP dose (Fig. 3), and the resulting dose dependence (Fig. 4) is similar to that obtained by fluorescent labeling (42–44). However, as discussed in the Introduction, shape change does not completely correlate with appearance of activation-specific receptors. Therefore, a combination of the new method and standard labeling techniques may provide deeper insight into the molecular mechanisms of platelet activation. The results of Figure 4 demonstrate good agreement between experiment and mathematical model, and the determined equilibrium constant is close to the value of $(10.9 \pm 1.8)\times10^{-8}$ M, reported for binding of ADP and $P2Y_1$ (35). This agrees with the accepted notion that ligand-receptor binding is the first stage of platelet activation by ADP.

To conclude, we proposed a novel method of precise and rapid determination of platelet volume and shape index, which allows detailed characterization of platelets without any fluorescent labels or additional reagents. Incorporation of this method into routine hematological analysis would provide new opportunities both for diagnosis of hemostatic disorders and for the development of novel therapeutic strategies. From biophysical viewpoint, rapid measurement of platelet shape is complimentary to other methods, and enables further studies of shape change mechanisms. For instance, importance of cytoskeleton components in this process can be assessed by using selective inhibitors such as taxol and cytochalasin (45–48).

Acknowledgments

D.I.S. also acknowledge the support by the Stipend of the President of Russian Federation for young scientists.

Literature Cited

1. Michelson AD. Preface. In: Platelets, 3rd ed. Academic Press; 2013. p xvii
2. Trowbridge EA, Reardon DM, Hutchinson D, Pickering C. The routine measurement of platelet volume: A comparison of light-scattering and aperture-impedance technologies. Clin Phys Physiol Meas 1985;6:221–238.
3. D'Souza C, Briggs C, Machin SJ. Platelets. Clin Lab Med 2015;35:123–131.
4. Briggs C, Kunka S, Hart D, Oguni S, Machin SJ. Assessment of an immature platelet fraction (IPF) in peripheral thrombocytopenia. Br J Haematol 2004;126:93–99.
5. Ault KA, Rinder HM, Mitchell J, Carmody MB, Vary CPH, Hillman RS. The significance of platelets with increased RNA content (reticulated platelets) a measure of the rate of thrombopoiesis. Am J Clin Pathol 1992;98:637–646.
6. Tycko DH, Metz MH, Epstein EA, Grinbaum A. Flow-cytometric light scattering measurement of red blood cell volume and hemoglobin concentration. Appl Opt 1985;24:1355–1365.
7. Maltsev VP. Scanning flow cytometry for individual particle analysis. Rev Sci Instrum 2000;71:243–255.
8. Moskalensky AE, Yurkin MA, Konokhova AI, Strokotov DI, Nekrasov VM, Chernyshev AV, Tsvetovskaya GA, Chikova ED, Maltsev VP. Accurate measurement of volume and shape of resting and activated blood platelets from light scattering. J Biomed Opt 2013;18:017001.
9. Paul BZS, Daniel JL, Kunapuli SP. Platelet shape change is mediated by both calcium-dependent and -independent signaling pathways. J Biol Chem 1999;274:28293–28300.
10. Kuwahara M, Sugimoto M, Tsuji S, Matsui H, Mizuno T, Miyata S, Yoshioka A. Platelet shape changes and adhesion under high shear flow. Arterioscler Thromb Vasc Biol 2002;22:329–334.
11. Ruf A, Patscheke H. Flow cytometric measurement of the platelets shape change. Thromb Haemost 1993;69:702.
12. Maurer-Spurej E, Chipperfield K. Past and future approaches to assess the quality of platelets for transfusion. Transfusion Med Rev 2007;21:295–306.

13. Milton JG, Frojmovic MM. Turbidometric evaluations of platelet activation: Relative contributions of measured shape change, volume, and early aggregation. J Pharmacol Methods 1983;9:101–115.
14. Born GV, Dearnley R, Foulks JG, Sharp DE. Quantification of the morphological reaction of platelets to aggregating agents and of its reversal by aggregation inhibitors. J Physiol (Lond) 1978;280:193–212.
15. Frojmovic MM, Panjwani R. Geometry of normal mammalian platelets by quantitative microscopic studies. Biophys J 1976;16:1071–1089.
16. Litvinov RI, Vilaire G, Shuman H, Bennett JS, Weisel JW. Quantitative analysis of platelet v 3 binding to osteopontin using laser tweezers. J Biol Chem 2003;278: 51285–51290.
17. Kroll MH, Afshar-Kharghan V. Platelets in pulmonary vascular physiology and pathology. Pulm Circ 2012;2:291–308.
18. Kestin AS, Ellis PA, Barnard MR, Errichetti A, Rosner BA, Michelson AD. Effect of strenuous exercise on platelet activation state and reactivity. Circulation 1993;88: 1502–1511.
19. Strokotov DI, Moskalensky AE, Nekrasov VM, Maltsev VP. Polarized light-scattering profile-advanced characterization of nonspherical particles with scanning flow cytometry. Cytometry A 2011;79:570–579.
20. Moskalensky AE, Strokotov DI, Chernyshev AV, Maltsev VP, Yurkin MA. Additivity of light-scattering patterns of aggregated biological particles. J Biomed Opt 2014;19: 085004.
21. Gilev KV, Yurkin MA, Chernyshova ES, Strokotov DI, Chernyshev AV, Maltsev VP. Mature red blood cells: From optical model to inverse light-scattering problem. Biomed Opt Express 2016;7:1305–1310.
22. Orlova DY, Yurkin MA, Hoekstra AG, Maltsev VP. Light scattering by neutrophils: Model, simulation, and experiment. J Biomed Opt 2008;13:054057.
23. Strokotov DI, Yurkin MA, Gilev KV, van Bockstaele DR, Hoekstra AG, Rubtsov NB, Maltsev VP. Is there a difference between T- and B-lymphocyte morphology? J Biomed Opt 2009;14:064036.
24. Konokhova AI, Gelash AA, Yurkin MA, Chernyshev AV, Maltsev VP. High-precision characterization of individual E. coli cell morphology by scanning flow cytometry. Cytometry A 2013;83:568–575.
25. Konokhova AI, Chernova DN, Moskalensky AE, Strokotov DI, Yurkin MA, Chernyshev AV, Maltsev VP. Super-resolved calibration-free flow cytometric characterization of platelets and cell-derived microparticles in platelet-rich plasma: Super-resolved characterization of plasma cells. Cytometry A 2016;89: 159–168.
26. Harrison P, Mackie I, Mumford A, Briggs C, Liesner R, Winter M, Machin S. British Committee for Standards in Haematology. Guidelines for the laboratory investigation of heritable disorders of platelet function. Br J Haematol 2011;155: 30–44.
27. Kolesnikova IV, Potapov SV, Yurkin MA, Hoekstra AG, Maltsev VP, Semyanov KA. Determination of volume, shape and refractive index of individual blood platelets. J Quant Spectrosc Radiat Transf 2006;102:37–45.
28. Paulus J. Platelet size in man. Blood 1975;46:321–336.
29. Ahnadi CE, Chapman ES, Lépine M, Okrongly D, Pujol-Moix N, Hernández A, Boughrassa F, Grant AM. Assessment of platelet activation in several different anticoagulants by the Advia 120 Hematology System, fluorescence flow cytometry, and electron microscopy. Thromb Haemost 2003;90:940–948.
30. Yurkin MA, Hoekstra AG. The discrete-dipole-approximation code ADDA: Capabilities and known limitations. J Quant Spectrosc Radiat Transf 2011;112:2234–2247.
31. Park Y, Schoene N, Harris W. Mean platelet volume as an indicator of platelet activation: Methodological issues. Platelets 2002;13:301–306.
32. Li J. Development and evaluation of flexible empirical peak functions for processing chromatographic peaks. Anal Chem 1997;69:4452–4462.
33. Konokhova AI, Rodionov AA, Gilev KV, Mikhaelis IM, Strokotov DI, Moskalensky AE, Yurkin MA, Chernyshev AV, Maltsev VP. Enhanced characterisation of milk fat globules by their size, shape and refractive index with scanning flow cytometry. Int Dairy J 2014;39:316–323.
34. Hantgan RR. A study of the kinetics of ADP-triggered platelet shape change. Blood 1984;64:896–906.
35. Baurand A, Raboisson P, Freund M, Léon C, Cazenave J-P, Bourguignon J-J, Gachet C. Inhibition of platelet function by administration of MRS2179, a P2Y1 receptor antagonist. Eur J Pharmacol 2001;412:213–221.
36. Gear AR. Rapid platelet morphological changes visualized by scanning-electron microscopy: Kinetics derived from a quenched-flow approach. Br J Haematol 1984; 56:387–398.
37. Girshovitz P, Shaked NT. Generalized cell morphological parameters based on interferometric phase microscopy and their application to cell life cycle characterization. Biomed Opt Exp 2012;3:1757–1773.
38. Chernyshev AV, Tarasov PA, Semianov KA, Nekrasov VM, Hoekstra AG, Maltsev VP. Erythrocyte lysis in isotonic solution of ammonium chloride: Theoretical modeling and experimental verification. J Theoretical Biol 2008;251:93–107.
39. Diagouraga B, Grichine A, Fertin A, Wang J, Khochbin S, Sadoul K. Motor-driven marginal band coiling promotes cell shape change during platelet activation. J Cell Biol 2014;204:177–185.
40. Sadoul K. New explanations for old observations: Marginal band coiling during platelet activation. J Thromb Haemost 2015;13:333–346.
41. Lippi G, Ippolito L, Zobbi V, Sandei F, Favaloro EJ. Sample collection and platelet function testing: Influence of vacuum or aspiration principle on PFA-100 test results. Blood Coagul Fibrinolysis 2013;24:666–669.
42. Ruf A, Patscheke H. Flow cytometric detection of activated platelets: Comparison of determining shape change, fibrinogen binding, and P-selectin expression. Semin Thromb Hemost 1995;21:146–151.
43. Shattil SJ, Cunningham M, Hoxie JA. Detection of activated platelets in whole blood using activation-dependent monoclonal antibodies and flow cytometry. Blood 1987; 70:307–315.
44. McEver RP, Martin MN. A monoclonal antibody to a membrane glycoprotein binds only to activated platelets. J Biol Chem 1984;259:9799–9804.
45. White JG. Influence of taxol on the response of platelets to chilling. Am J Pathol 1982;108:184–195.
46. White JG, de Alarcon PA. Platelet spherocytosis: A new bleeding disorder. Am J Hematol 2002;70:158–166.
47. Casella JF, Flanagan MD, Lin S. Cytochalasin D inhibits actin polymerization and induces depolymerization of actin filaments formed during platelet shape change. Nature 1981;293:302–305.
48. Natarajan P, May JA, Sanderson HM, Zabe M, Spangenberg P, Heptinstall S. Effects of cytochalasin H, a potent inhibitor of cytoskeletal reorganisation, on platelet function. Platelets 2000;11:467–476.